

Wilfrid Laurier University

Scholars Commons @ Laurier

---

Mathematics Faculty Publications

Mathematics

---

2002

## Dynamics of Torque-Speed Profiles for Electric Vehicles and Nonlinear Models Based on Differential-Algebraic Equations

Roderick V.N. Melnik

*Wilfrid Laurier University, [rmelnik@wlu.ca](mailto:rmelnik@wlu.ca)*

Ningning Song

*University of Southern Denmark*

Per Sandholdt

*Sauer-Danfoss A/S*

Follow this and additional works at: [https://scholars.wlu.ca/math\\_faculty](https://scholars.wlu.ca/math_faculty)

---

### Recommended Citation

Melnik, Roderick V.N.; Song, Ningning; and Sandholdt, Per, "Dynamics of Torque-Speed Profiles for Electric Vehicles and Nonlinear Models Based on Differential-Algebraic Equations" (2002). *Mathematics Faculty Publications*. 37.

[https://scholars.wlu.ca/math\\_faculty/37](https://scholars.wlu.ca/math_faculty/37)

This Article is brought to you for free and open access by the Mathematics at Scholars Commons @ Laurier. It has been accepted for inclusion in Mathematics Faculty Publications by an authorized administrator of Scholars Commons @ Laurier. For more information, please contact [scholarscommons@wlu.ca](mailto:scholarscommons@wlu.ca).

## DYNAMICS OF TORQUE-SPEED PROFILES FOR ELECTRIC VEHICLES AND NONLINEAR MODELS BASED ON DIFFERENTIAL-ALGEBRAIC EQUATIONS

RODERICK V.N. MELNIK AND NINGNING SONG

University of Southern Denmark  
MCI, Faculty of Science and Engineering,  
Sonderborg, DK-6400, Denmark

PER SANDHOLDT

Sauer-Danfoss A/S, Nordborg, Denmark

**Abstract.** The so-called  $\mu - \lambda$  curves, where  $\lambda$  is the slip ratio and  $\mu$  is the normalised traction force or the friction index, are nonlinear functions of the velocity of the vehicle and the wheel rotational velocity. Despite their predominant use in the literature, linear approximations of such curves may fail to predict correctly key characteristics of vehicle performance efficiency such as torque-speed profiles. Although attempts to model these characteristics in the context of slip phenomena have been made before, to our best knowledge a general model with respect to the vehicle velocity, the wheel rotating velocity, the slip ratio, the traction force, and the torque, has never been formulated and solved as a coupled nonlinear problem based on a system of differential-algebraic equations arising naturally in this context. In this paper, such a model is formulated, solved numerically, and some results of numerical simulation of driving an electric vehicle on different surface conditions are presented.

**1. Introduction.** A current trend in finding efficient alternatives to conventional internal combustion engine vehicles, a major source of urban pollution, brings along a number of challenging problems for applied mathematicians. In this paper we are interested in the analysis of performance efficiency of electric vehicles (EV). In addition to environmental and energy advantages (e.g., [16]), such vehicles have an impressive potential in terms of new engineering solutions. Indeed, torque in such vehicles can be generated very fast and accurately for both accelerating and decelerating modes, while a motor can be attached to each wheel allowing an easier control of the vehicles.

It is well known that a key measure of efficiency of electric vehicles is their torque-speed profiles (e.g., [2]). In order to construct such profiles, it is important to be able to model *nonlinear* slip phenomena of a wheel. Major difficulties in the solution of this problem are coming from a complex character of dependencies between the normalised traction force (or the friction index)  $\mu$  and the slip ratio  $\lambda$ , not known a priori, but rather estimated experimentally for typical surface conditions. In what follows we propose a model based on a system of differential-algebraic equations that allows us to quantify nonlinear slip phenomena of a wheel. The system links together the vehicle velocity, the wheel rotating velocity, the slip ratio, the traction force, and the torque in a one single system which is solved numerically by using

---

1991 *Mathematics Subject Classification.* 37M05,65P40,65L80 .

*Key words and phrases.* Nonlinear slip phenomena, differential-algebraic models.

a differential-algebraic solver. We organise this paper as follows. In Section 2 we formulate a coupled system of differential equations describing the wheel and vehicle dynamics and specify an algebraic equation for the dependency of the velocities on the torque. In Section 3 we describe a nonlinear slip ratio model, and in Section 4 we present the fully coupled model describing electric vehicle dynamics. Representative examples of computational experiments are discussed in Section 5.

**2. Mathematical models for electric vehicle dynamics.** In order to describe the dynamics of electric vehicles we need to couple the vehicle velocity with the wheel rotational velocity via characteristics of the motor and surface such as the traction force, the torque, etc. We start our discussion from an equation governing the dynamics of the vehicle.

**2.1. Vehicle motion model.** The motion of the vehicle is described in terms of its longitudinal speed as

$$I_v dV/dt = \bar{F}_d(t, \lambda) - \bar{F}_{\text{aerod}} - \bar{F}_{\text{gravity}} - \bar{F}_{\text{rolling}}, \quad (1)$$

where  $V$  is the vehicle velocity, and  $\lambda$  is the slip ratio. The gravity force,  $\bar{F}_{\text{gravity}}$ , and the rolling resistance,  $\bar{F}_{\text{rolling}}$ , are

$$\bar{F}_{\text{gravity}} = M \sin(\alpha), \quad \bar{F}_{\text{rolling}} = M(\mu \cos(\alpha) + \tilde{\mu}V), \quad (2)$$

where  $\alpha$  is the road/surface angle,  $\mu$  characterises the road surface for a particular wheel, so that it can be understood as the friction coefficient between wheel and road, and  $\tilde{\mu}$  is the friction coefficient for wheel mechanism that accounts for friction in the wheel bearings and other speed-dependent retarding torques (e.g., [1]). As pointed out in [1], the road surface cannot be characterised independently of the wheel because the rolling resistance of a particular surface also depends on wheel specific factors, e.g. tire pressure, thread type, etc. Other functions to be defined in (1) are the aerodynamic drag,  $\bar{F}_{\text{aerod}}$ , the vehicle inertia,  $I_v$ , and the normalised traction force,  $\bar{F}_d(t, \lambda)$ . The first of the above quantities is defined as follows (e.g., [5, 1])

$$\bar{F}_{\text{aerod}} = C_d A_d \rho \text{sgn}(V - \bar{V}_w)(V - \bar{V}_w)^2, \quad (3)$$

where  $A_d$  is the cross-sectional area constant pertinent to the drag,  $\rho$  is the air density,  $C_d$  is the specific aerodynamic drag coefficient, and  $\bar{V}_w$  is the wind speed in the direction of the vehicle's motion. We note that aerodynamic resistance is not a significant factor as long as we deal with off-road vehicles operating under 48 km/h [15]. The rotational inertia of the wheels and the electric motor is taken into account in the acceleration term by using the effective mass of the vehicle

$$I_v = M/g + f(n_w, r_w, I_w, I_m), \quad (4)$$

where  $f$  is a function of the number of the wheel ( $n_w$ ), radius of the wheel ( $r_w$ ), rotational inertia of the wheel ( $I_w$ ), and the electric motor ( $I_m$ ). An explicit approximation to  $f$  can be found in [1]. A generalisation of the model to the many-wheel scenario can also be considered [14, 15]. Finally, we define the normalised traction force via the relationship

$$F_d = \mu(\lambda)N, \quad 0 \leq \lambda \leq 1, \quad (5)$$

where  $N$  is the normal force defined on the flat surfaces as  $N = Mg$  (here  $\bar{F}_d = F_d/g$ ).

Our main interest here is in off-road vehicles, in particular those that are designed for traction. Specifically, we are interested in modelling the dynamics of electric greens mowers, e.g. Ransomes E-Plex II type electric vehicles. In this case, for the flat surface situation system (1)–(5) is reduced to

$$MdV/dt = F_d(t, \lambda), \quad (6)$$

where the key to understanding of vehicle dynamics is kept by  $F_d$ . Note that we include here the full nonlinear dependency on  $\lambda$  in the tire driving force. Some simplified models are known in the literature where instead of  $\lambda$  one defines another parameter attempting to exclude from the definition of  $\lambda$  the wheel radius [5]. However, in typical analyses of the situation considered so far in the literature (e.g. [10, 11]) the model (1)–(5) is linearised with respect to the slip ratio which is defined as

$$\lambda = 1 - V/V_w, \quad V_w \geq V; \quad \lambda = V_w/V - 1, \quad V \geq V_w, \quad (7)$$

where  $V_w = r\omega$  is the velocity of the wheel,  $r$  is the wheel radius (assumed here constant), and  $\omega$  is the angular velocity. From a physical point of view the situation in (7) where  $V_w \geq V$  corresponds to the accelerating wheel, while  $V \geq V_w$  corresponds to the decelerating wheel.

**2.2. Model for the wheel dynamics.** For the wheel dynamics we have

$$I_w dV_w/dt = K_g K_T (\delta - K_g \varphi) - B_w V_w - F_d(t, \lambda), \quad (8)$$

where  $I_w$  is the wheel inertia, and  $B_w$  is used to account for the speed-dependent friction-force against the wheel shaft motion. Before proceeding further with specification of parameters in (8), we note that in the most general setting this equation should be coupled to the evolution equation for the motor shaft speed ( $n$ ) which can be written as follows

$$I_m dn/dt = g(n, B_m, K_T, K_g, \delta, \varphi, T_e, u), \quad (9)$$

where  $B_m$  is the parametrised characteristic of the speed-dependent friction-force for the motor shaft,  $K_T$  is the torsional stiffness of the transmission which provides coupling between the motor and the wheel by the gear ratio  $K_g$ . In (9)  $T_e$  is the motor torque before the reduction,  $\varphi$  (determined from  $d\varphi/dt = V_w$ ) is the wheel position, and  $\delta$  (determined from  $d\delta/dt = n$ ) is the motor shaft position. In the context of off-road vehicles, system (8)–(9) can be simplified to

$$M_w dV_w/dt = F_m - F_d(t, \lambda), \quad (10)$$

where  $F_m$  is the force generated by engine, that is in our case by the motor torque. Following [11], we consider here a one-wheel model. Further, we note that for the electric vehicles of interest the motor torque can be determined from the relationships connecting it with the power,  $P$ , and the wheel velocity

$$F_m = T_w/r_w, \quad \text{where} \quad T_w = P/\omega, \quad \omega = V_w/r_w, \quad (11)$$

and  $T_w$  is the wheel torque. In the case of Ransomes E-Plux II, the power is supplied by a 48V battery, and the input power to the mower as a function of current  $i_a$  can be written as

$$P = k_t \omega i_a = k_t \frac{V_w}{r} i_a, \quad (12)$$

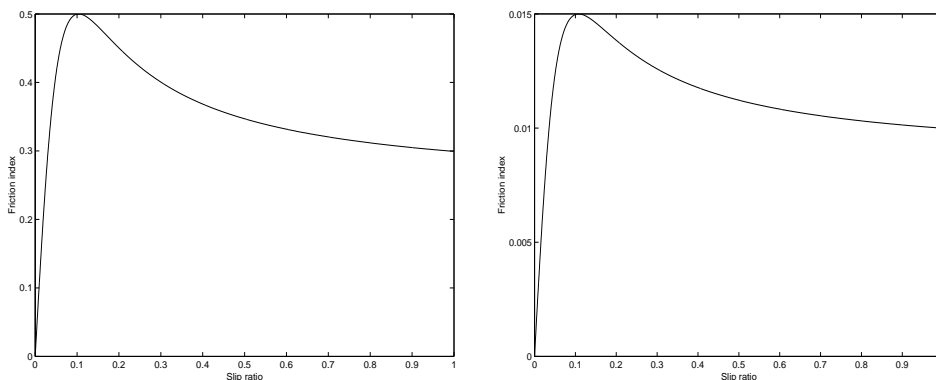


FIGURE 1. Approximating  $\mu - \lambda$  curves for dry (left) and wet (right) grass.

where  $i_a$  is the supplied current. For simplicity the torque constant ( $k_t$ ) was set to 1 in experiments reported below. Gear ratio and the total moment of inertia are implemented into the model in a straightforward manner.

**3. Nonlinear slip ratio models.** Constructing realistic models for the slip ratio is known to be a difficult problem [6]. At the same time, this problem, often discussed in the context of the tire-road friction estimation techniques, becomes the subject of one of the most important research areas in modelling the vehicle dynamics. The basis for most of the existing methodologies lies with the assumption that the slip ratio,  $\lambda$ , (sometimes called the slope or longitudinal stiffness) is sufficient to provide an accurate estimate for the friction,  $\mu$ . A number of different approximations for  $\mu(\lambda)$  curves have been proposed in the literature [15, 7]. Rational polynomial approximations such as  $\mu = k\lambda/(a\lambda^2 + b\lambda + 1)$  are among those most frequently used ( $k$ ,  $a$  and  $b$  are given constants). However, such approximations lead to a non-zero slip when the traction force is zero, so that the slip computed from the such approximations gives a significant offset. Although this fact has been already discussed in the literature (e.g., [3]), most of the models are still based on the linear approximation  $\lambda = \mu/k$ . In this paper we use the following approximation for the  $\mu - \lambda$  curve

$$\mu = \mu_0 \sin \left\{ \mu_1 \arctan \left[ \mu_2(1 - \mu_3)\lambda + \frac{\mu_3}{\mu_2} \arctan(\mu_2\lambda) \right] \right\}. \quad (13)$$

This dependency reproduces very well all surface conditions we have had to deal with in this project. Based on Sauer-Danfoss data for different surfaces of interest, we found that for all of them we can choose  $\mu_1 = 22$  and  $\mu_3 = 1$ . The other two coefficients in (13) can be chosen as specified in Table 1. The  $\mu - \lambda$  curves for dry and wet grass are plotted in Fig. 1. There is substantial evidence to suggest that the data quality is effectively assessed by the variation in  $\mu(t)$  [3]. The methodology we have developed in this paper provides a consistent and systematic approach to constructing  $\mu(t)$ .

**4. Nonlinear models for EV dynamics based on differential-algebraic equations.** As we have already mentioned, most models proposed in the literature so far in the context of constructing torque-speed profiles are based on simplified,

Surface type	Dry grass	Sand	Ice	Wet grass
$\mu_0$	0.5	0.35	0.25	0.015
$\mu_2$	13.0965	12.93	11.95	13.6

TABLE 1. Approximating  $\mu - \lambda$  curves: coefficients for typical surface conditions.

typically linear models (e.g., [11] and references therein). Ultimately, in such models the dynamics of the wheel and of the vehicle can be uncoupled precluding a systematic treatment of realistic surface conditions. On the contrary, the approach proposed in this paper allows us to deal with the coupling of the velocities via the torque, slip ratio, and the traction force. Summarising the discussion of Sections 1–3 and denoting  $y_1 \equiv V_w$ ,  $y_2 \equiv V$ ,  $y_3 \equiv \lambda$ ,  $y_4 \equiv \mu$ ,  $y_5 \equiv P$ , we arrive at the following system of differential-algebraic equations

$$\left\{ \begin{array}{l} \frac{dy_1}{dt} = \frac{1}{M_w} \left( \frac{y_5}{y_1} - y_4 M g \right), \quad \frac{dy_2}{dt} = \frac{1}{M} y_4 g M_w, \\ 0 = -y_4 + \mu_0 \sin \left\{ \mu_1 \arctan \left[ \mu_2 (1 - \mu_3) y_3 + \frac{\mu_3}{\mu_2} \arctan(\mu_2 y_3) \right] \right\}, \\ 0 = -y_3 + \min \left( \left| 1 - \frac{y_2}{y_1} \right|, \left| 1 - \frac{y_1}{y_2} \right| \right), \quad 0 = -y_5 + \frac{y_1}{r} i_a. \end{array} \right. \quad (14)$$

If we denote a vector of differential variables by  $x$ , and the vector of algebraic variables by  $z$ , system (14) can be cast in the general form of semi-explicit differential-algebraic (DAE) models

$$x' = f(x, z, t), \quad \& \quad g(x, z, t) = 0 \quad (15)$$

with the general solution represented in terms of  $y^T = [x^T z^T]$ . The degree of singularity of (15) is linked to nilpotency of the associated matrix pencils (e.g., [4]). System (14) has been analysed numerically by using three algorithms, the Gear backward differentiation formula, a modified Rosenbrock formula of order 2, and our own iterative scheme. The latter is based on a MATLAB-based time-adaptive algorithm with explicit verification of the condition on the maximum power. The system, which in its reduced form has index 1, has been solved for different situations of interest, providing further insight into key characteristics of the performance dynamics of electric vehicles. The results of computational experiments with some typical inputs are discussed in Section 5.

**5. Computational experiments.** In this section we present some results obtained from computational experiments with model (14) for off-road vehicle data, in particular for an electric triplex greens mower of the Ransome E-Plex type. This particular design is a three-wheel electric vehicle model (see also [12]). With appropriate modifications, the developed methodology can also be applied to other designs of electric vehicles (e.g., [13, 9]). The analysis of the dynamics has been carried out in conjunction with time-dependent torque/current profiles, an important characteristic in preventing slip phenomena. The following three groups of typical situations have been analysed

- pre-defined surface conditions (either wet or dry grass in each single experiment) for a pre-defined torque/current dynamics;

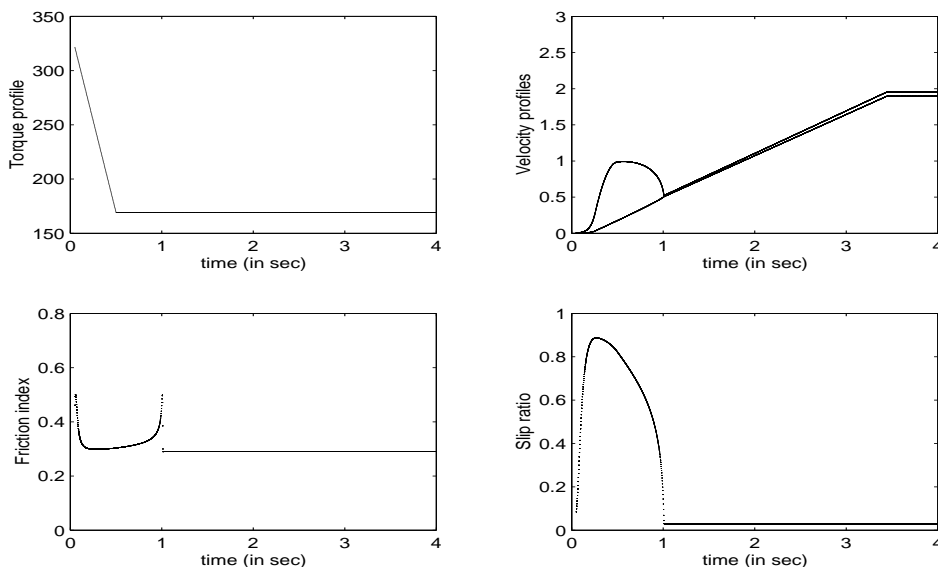


FIGURE 2. Dynamics of the vehicle on a flat dry grass surface.

- changing surface conditions (within a single experiment) for different torque dynamics;
- different topography of the surface, including uphill/downhill situations, as well as the general time-dependent angle situation.

In typical situations, torque-speed profiles for electric motors have constant-rate torque up to the so-called base angular velocity,  $\omega_{\text{base}}$ , at which the motor reaches its power limit. Then, the motor still operates with constant power up to the maximum angular velocity,  $\omega_{\text{max}}$ . In the case of the electric mower we consider in this paper, we have estimated the peak performance of the vehicle (e.g., [8]) at  $P_{\text{max}} = 1300\text{W}$ ,  $n_{\text{max}} = 146.78\text{rev/min}$ ,  $\omega_{\text{max}} = 15.37\text{rad/sec}$ ,  $\omega_{\text{base}} = 7.685\text{rad/sec}$ ,  $T_{w,\text{max}} = 169.2\text{Nm}$ , where  $n$  is the typical value for resolutions per minutes (for one wheel). Initial values for  $V$  and  $V_w$  in all experiments have been chosen so that they do not exceeded  $5 \times 10^{-3}$ . Other characteristics of the vehicle used in the computational experiments are  $M = 221.3\text{kg}$  (the mass of the vehicle is taken as one third of the total mass unit),  $M_w = 11.65\text{kg}$ ,  $g = 9.82\text{m/s}^2$ ,  $k_t = 1\text{Nm/A}$ ,  $r_w = 0.254\text{m}$ . As a first example, we consider the acceleration of the mower on dry grass. In this case two algebraic equations of the DAE model (14) are simplified to

$$\lambda = 1 - V/V_w, \quad \mu = \mu_0 \sin(\arctan(22/\mu_2 \arctan(\mu_2 \lambda))). \quad (16)$$

The results for  $i_a = \max(338.4(1 - t), 169.2)$  are shown in Fig. 2. As it is seen, we have to deal with a large initial slip ratio, up to 0.9 on a unit scale. The curve of the velocity of the wheel during this time is above the curve of the vehicle velocity, indicating severeness of slip phenomena. The situation changes after the slip ratio drops, and the wheel and vehicle velocities are maintained at the same level. Moving to a wet surface (after 2 seconds) will change this balance, as shown in Fig. 3. Changing the current/torque to a smoother (e.g., quadratic) profile would remedy the situation. In the presence of surface roughness, e.g. considering the vehicle operating on a golf course, for small angles the pattern of the uphill motion

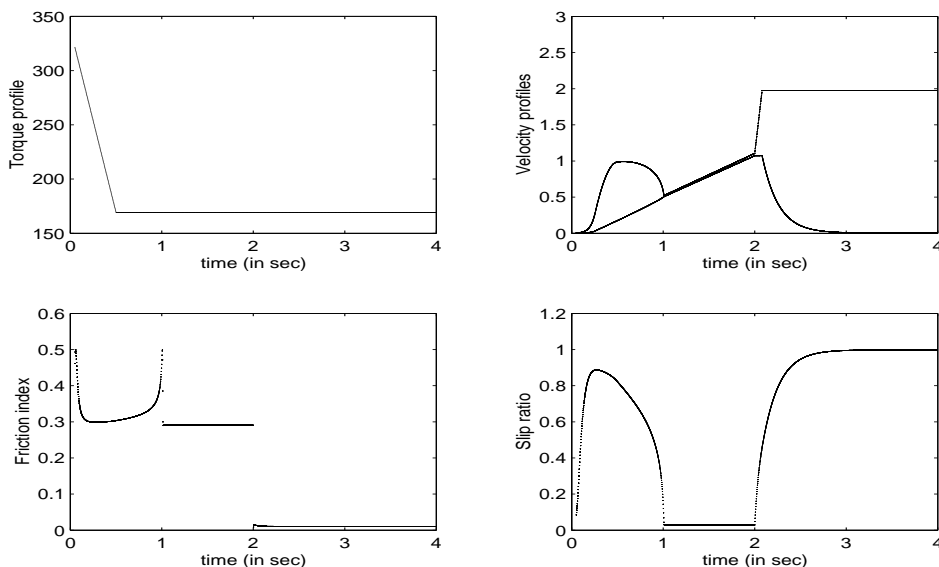


FIGURE 3. Dynamics of the vehicle on a flat surface with different properties.

is barely different from that already presented in Fig. 2. However, for sufficiently high angles the situation, even on a dry grass surface, can be similar to that depicted in Fig. 3. What is different in these situations is the sign of the vehicle gravitational force component, so that the traction force is defined in terms of the friction force  $F_r$  and  $F_{\text{inc}}$

$$F_d = F_r + F_{\text{inc}}, \quad F_r = \mu M G \cos \theta, \quad F_{\text{inc}} = M g \sin \theta. \quad (17)$$

Accordingly, two differential equations of system (14) are modified to account for additional force ( $F_{\text{inc}}$ )

$$\frac{dV_w}{dt} = \frac{1}{M_w} \left( \frac{P}{V_w} - (\mu M g \cos \theta - M g \sin \theta) \right), \quad \frac{dV}{dt} = \mu g \cos \theta - g \sin \theta, \quad (18)$$

while the algebraic equations of the model remain unchanged. The last term in both equations (18) changes its sign in the downhill motion which helps to maintain the velocity of the wheel and vehicle at the same level.

Not only the described model allows us to treat different surface conditions, it also allows us to treat different surface topographies. For example, in Fig. 4 we present the situation where, after 1 second of operation, the vehicle moves from a flat dry grass area to a changing topographic surface with  $\theta = 14 \sin(4(t-1))$ .

In conclusion, we note that although mathematically straightforward, the extension of our model to many wheel scenarios leads to several new challenges. In particular, handling characteristics of the vehicle and steering geometry may become quite important, while all forces, e.g. rolling resistances, tractive forces have to be included into consideration for both the front and rear wheels.

#### REFERENCES

- [1] Craparo, J.C. and Thacher, E.F., A solar-electric vehicle simulation code, *Solar Energy*, 55(3), 1995, 221–234.
- [2] Ehsani, M., Rahman, K.M., and Toliyat, H.A., Propulsion system design of electric and hybrid vehicles, *IEEE Trans. on Industrial Electronics*, 44, 1997, 19–27.

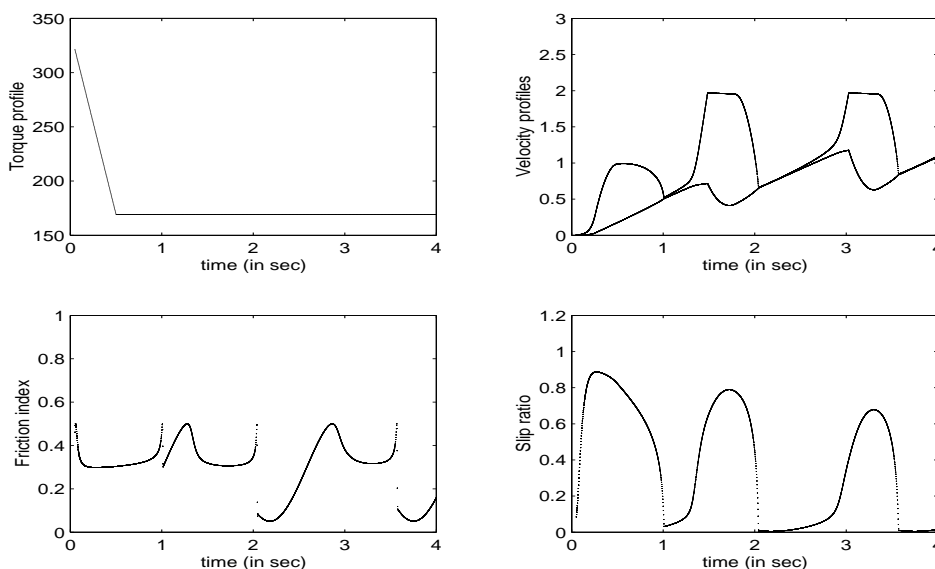


FIGURE 4. Dynamics of the vehicle on flat dry grass under changing topographical conditions.

- [3] Gustafsson, F., Slip-based tire-road friction estimation, *Automatica*, **33**, 1997, 1087–1099.
- [4] Hairer, E., Wanner, G., Solving ODEs II. Stiff and Differential-Algebraic Problems, Springer, 1996.
- [5] Haskara, I., Ozguner, U., and Winkelman, J., Wheel slip control for antispin acceleration via dynamic spark advance, *Control Engineering Practice*, **8**, 2000, 1135–1148.
- [6] Kataoka, H., et al, Optimal slip ration estimator for traction control system of electric vehicle based on fuzzy inference, *Electrical Engineering in Japan*, 135(3), 2001, 56–63.
- [7] Kiencke, U. and Daiss, A., Observation of lateral vehicle dynamics, *Control Eng. Practice*, **5**, 1997, 1145–1150.
- [8] Mizuno, T. et al, Basic principle and maximum torque characteristics of a six-phase pole change induction motor for electric vehicles, *Electrical Engineering in Japan*, 118(3), 1997, 78–91.
- [9] Sakai, S., Sado, H., Hori, Y., Motion control in an electric vehicle with four independently driven in-wheel motors, *IEEE-ASME Trans. on Mechatronics*, 4(1), 1999, 9–16.
- [10] Sakai, S-I., Sado, H., and Hori, Y., Novel skid detection method without vehicle chassis speed for electric vehicle, *JSAE Review*, **21**, 2000, 503–510.
- [11] Sakai, S., Hori, Y., Advanced motion control of EV with fast minor feedback loops: basic experiments using the 4-wheel motored EV “UOT Electric March II”, *JSAE Review*, 22, 2001, 527–536.
- [12] Solero, L., et al, Nonconventional three-wheel electric vehicle for urban mobility, *IEEE Trans. on Vehicular Technology*, 50(4), 2001, 1085–1091.
- [13] Terashima, M., et al, Novel motors and controllers for high-performance electric vehicle with four in-wheel motors, *IEEE Trans. on Industrial Electronics*, **44**, 1997, 28–38.
- [14] Thompson, D.E., Design Analysis. Mathematical Modeling of Nonlinear Systems, Cambridge University Press, 1999.
- [15] Wong, J.Y., Theory of Ground Vehicles, 3rd Ed., John Wiley & Sons, 2001.
- [16] Yan, X. and Patterson, D., Novel power management for high performance and cost reduction in an electric vehicle, *Renewable Energy*, **22**, 2001, 177–183.

Received September 2002; in revised March 2003.

E-mail address: rmelnik@mci.sdu.dk